FEDSM2007-37562

CAVITATION IN KÁRMÁN VORTEX SHEDDING FROM 2D HYDROFOIL: WALL ROUGHNESS EFFECTS

Philippe Ausoni   Mohamed Farhat   François Avellan

Ecole Polytechnique Fédérale de Lausanne
Laboratory for hydraulic machines
Av. Cour 33bis, CH-1007 Lausanne
Switzerland

ABSTRACT

The present study deals with the shedding process of the Kármán vortices in the wake of a NACA0009 hydrofoil at high Reynolds number, $Re_h=25 \cdot 10^3 - 65 \cdot 10^3$. This research addresses the effects of the foil leading edge roughness on the wake dynamic with a special focus on the vortex shedding frequency, vortex-induced vibration and three-dimensionality of vortex shedding.

For smooth leading edge, the shedding frequency of Kármán vortices occurs at constant Strouhal number, $St=0.24$. The wake exhibits 3D instabilities and the vortex induced vibration signals strong modulation with intermittent weak shedding cycles. Direct relation between vibration amplitude and vortex spanwise organization is shown. In the case of rough leading edge, the Kármán shedding frequency is notably decreased compared to the smooth one, $St=0.18$. Moreover, the vortex induced vibration level is significantly increased and the vibration spectra sharply peaked. The occurrence of vortex dislocations is shown to be less frequent with the roughness. The shedding of the vortices is considered on the whole as in phase along the hydrofoil span.

Obviously, the shedding process of the Kármán vortices is highly related to the state of the boundary layer over the entire hydrofoil. It is believed that in the case of smooth leading edge, slight spanwise non-uniformities in the boundary-layer flow lead to slight instantaneous variation in vortex shedding frequency along the span which is enough to trigger vortex dislocations. On the contrary, for the rough leading edge, the location of transition to turbulence is uniformly forced which leads to the reduction of the spanwise boundary-layer non-uniformities and therefore to the enhancement of the coherence length of the Kármán vortices.

NOMENCLATURE

b	Hydrofoil span [m]	
C_{ref}	Reference velocity at the test section inlet [m/s]	
f_s	Vortex shedding frequency [Hz]	
f_t	Hydrofoil torsion eigen frequency [Hz]	
l	Hydrofoil chord length [m]	
p_{inlet}	Reference pressure at the test section inlet [bar]	
p_v	Vapour pressure [bar]	
Re_h	Reynolds number [-]	$Re_h=C_{ref}h/\upsilon$
St	Strouhal number [-]	$St=f_s h/C_{ref}$
$Stdv_{signal}$	Signal standard deviation	

$$Stdv_{signal} = \sqrt{\sum_{i=1}^{N}(x_i - \bar{x})^2 \Big/ N}$$

h	Hydrofoil trailing edge thickness [m]	
α	Incidence angle of the hydrofoil [°]	
σ	Cavitation index [-]	$\sigma=2(p_{inlet}-p_v)/\rho C_{ref}^2$
σ_i	Cavitation inception index [-]	
υ	Kinematic viscosity [m²/s]	

INTRODUCTION

Experimental studies on vortex shedding in the wake of bluff bodies have most often been conducted in laminar flows as a consequence of the interest in this fundamental flow. In many applications however, the flow fields in which bodies are immersed are turbulent. It is known that the introduction of turbulence to the flow field promotes the vortex shedding critical transition at lower Reynolds numbers than it is the case in laminar flows, and that increasing the surface roughness of the body has a similar effect, Achenbach and Heinecke [1]. The effect of surface roughness at higher Reynolds numbers is less clear, partly due the lack of experimental data. It is shown that the vortex shedding frequency is drastically decreased for rough cylinders in comparison with very smooth surface [1]. Wind-tunnel study shows that the introduction of free-stream turbulence acted to increase cylinder lift coefficients above those for laminar flow, Cheung and Melbourne [2]. Blackburn and Melbourne [3] examine the effects of grid-generated turbulence on lift forces at sections of a circular cylinder. According to spectra and correlation length analysis, it is thought that the increase of the mean flow turbulence intensity promotes the re-establishment of organized vortex shedding.

When the pressure is low enough, bubbles filled with vapor and non condensable gas are initiated and persist in the centre of individual shed vortices. Young and Holl [4] investigate the case of a flow around wedges and observe that the cavitation development in the wake increases the vortex shedding frequency by up to 25% and therefore affects the dynamic of the Kármán street. Ausoni *et al*. [5] confirms these results in the case of a 2D hydrofoil and analyze the cavitation effects on the vortex street morphology: Comparison of instantaneous velocity fields in cavitation free regime and high speed visualization of vortices cavitation does not show notable influence of the cavitation on the vortex street morphology. In terms of vortex coherent length, cavitation can therefore be considered as a passive agent of wake structure visualization. Ausoni *et al*. [6] investigate the cavitation influence on Kármán vortex shedding and induced hydrofoil vibrations. For the cavitation inception index, a new relationship is proposed and validated. In contrast to the earlier models, the new correlation takes into account the trailing edge displacement velocity. In addition, it is found that the transverse velocity of the trailing edge increases the vortex strength linearly.

In this paper, we describe a series of water-tunnel experiments with a fixed 2D hydrofoil and in which the Reynolds number is varied from $25 \cdot 10^3$ to $65 \cdot 10^3$. For two different leading edge roughnesses, vortex-induced vibrations are measured and comparisons are made in terms of vortex shedding frequency and vibration amplitude. Cavitation is used as a mean of visualization of the wake flow: Since vortex-induced vibration and high speed visualization are synchronized, the hydrofoil vibration level is considered versus the vortex spanwise instabilities and the occurrence of the 3D structures of shed vortices is investigated.

EXPERIMENTAL SETUP

The EPFL high-speed cavitation tunnel, outlined on Figure 1, is a closed loop with a test section of 150x150x750 mm, Avellan *et al*. [7]. The operating flow parameters are the upstream velocity C_{ref}, the cavitation index σ and the hydrofoil incidence angle α.
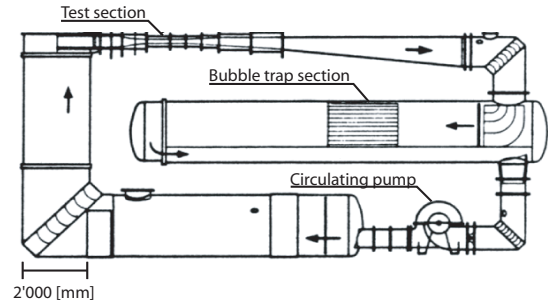

Figure 1 : EPFL high speed cavitation tunnel

The experimental 2D hydrofoil, sketched on Figure 2, is a blunt truncated Naca0009 made of stainless steel. The trailing edge thickness h is 3.22 mm and its chord length L and span b are 100 mm and 150 mm respectively. The hydrofoil mounting in the test section can be considered as a perfect embedding on one side and pivot embedding on the other. For all the measurements, the incidence angle of the hydrofoil α is fixed at 0° and the cavitation index is set high enough to allow cavitation occurrence only in the wake and not on the hydrofoil surface.

Caron [8] evidences that the boundary layer transition to turbulence for this hydrofoil geometry is located slightly downstream of the midchord for an incidence angle of 0° and Reynolds number Re_h between $42 \cdot 10^3$ and $70 \cdot 10^3$. Ait Bouziad [9] reports boundary layer computations and evaluates its thickness at the leading edge, $\delta \sim 100\mu m$. In order to investigate the wall roughness effects on the vortex shedding process, a distributed roughness made of glue and 125μm diameter sand are placed on both side of the hydrofoil 4 mm behind the leading edge, Figure 2. Therefore, for such a configuration, the transition to turbulence is uniformly forced. In the rest of the article, this configuration will be designated *rough*. In contrast, the case without rough stripes will be designated *smooth*.
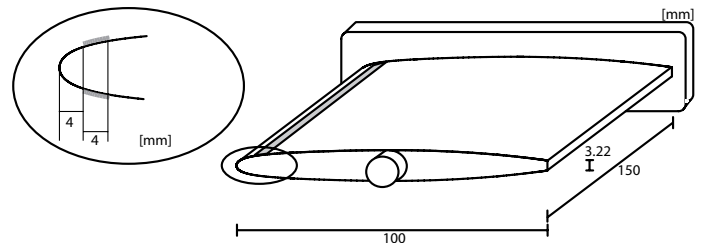

Figure 2 : Blunt truncated Naca 0009 hydrofoil and rough stripes at leading edge

The flow induced hydrofoil vibrations are measured with the help of a laser vibrometer. The measurement principle of the device is based on the detection of the frequency shift of the reflected laser beam according to the Doppler effect; the frequency shift being directly related to the displacement velocity of the surface in the laser direction. The location of the vibration amplitude measurements points is shown in Figure 3. Laser vibrometer measurements are synchronized with an accelerometer which is fitted on the profile support. By using the accelerometer signal as the reference one, the amplitude and phase of the hydrofoil motion at each measurement point are obtained and the eigen modes identified for the detected hydro-elastic couplings.

The data acquisition system has 16 bits A/D resolution, 16 inputs, a memory depth of 1 MSamples/Channel and a maximum sampling frequency of 51.2 kHz/Channel.

The vortical structures in the wake are visualized with the help of a high speed digital camera. The CCD image resolution is 512x256 pixels at 12'500 frames/sec.
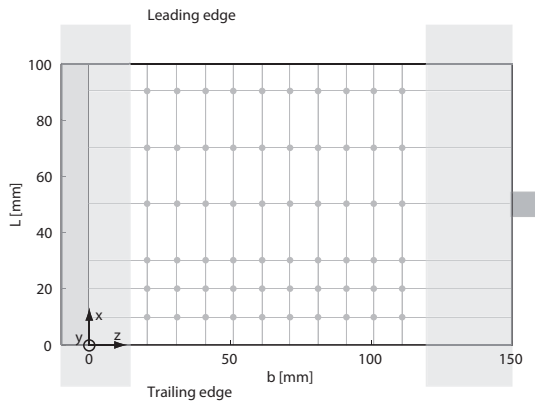

Figure 3 : Location of the hydrofoil vibration amplitude measurements points

FLUID-STUCTURE INTERACTION FOR SMOOTH LEADING EDGE

The waterfall spectra of the laser vibrometer signals is presented in Figure 4 for different upstream velocities. Most of the spectral energy is concentrated around the Kármán shedding frequency which increases linearly with the upstream velocity. The amplitude of the induced vibration changes according to the upstream velocity: As the vortex shedding frequency approaches one of the natural frequencies of the combined fluid-structure system, the coupling takes place with a significant increase of the vibration level. The vortex shedding frequency is "locked" onto the structural eigen frequency which is 900 Hz for flow velocity ranging from 11 to 13 m/s, i.e. $Re_h = 35 \cdot 10^3$ to $42 \cdot 10^3$.
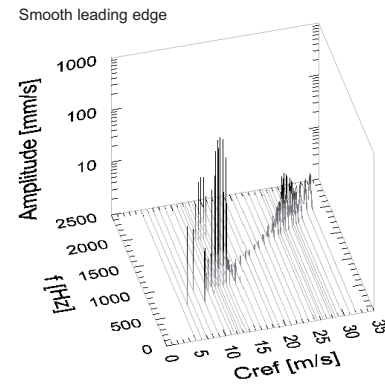

Figure 4 : Waterfall spectra of the laser vibrometer signals for different upstream velocities, cavitation free

The vortex shedding frequency normalized by the lock-in frequency and calculated from the laser vibrometer signal is presented in Figure 5 as a function of the flow velocity. A linear relationship between the vortex shedding frequency and the upstream velocity is observed provided that no hydrofoil resonance frequencies are excited. For such lock-off regime, the generation process of Kármán vortices occurs at constant Strouhal number, St=0.24. The hydrofoil trailing edge vibration amplitude at the vortex shedding frequency is also evidenced in Figure 5. In lock-in conditions corresponding to 11-13 m/s upstream velocities, we observe the increase and decrease of the vibration amplitude.
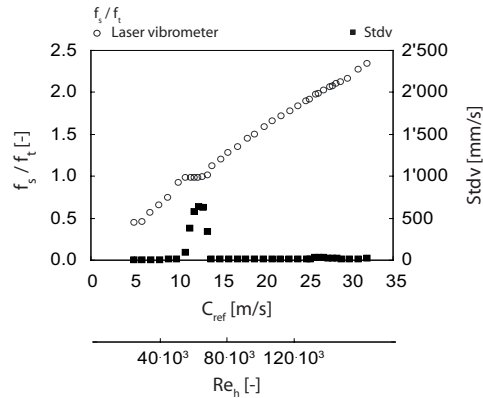
Figure 5 : Shedding frequency of Kármán vortices and vibration amplitude of the hydrofoil trailing edge for different upstream velocities, cavitation free

For the above mentioned lock-in condition, the hydrofoil wall vibration is surveyed by laser vibrometer measurements. As illustrated in Figure 6, the modal shape is identified as the 1st torsion mode. The maximum vibration amplitude of the trailing edge is up to $0.2 \cdot 10^{-3}$ m. For this condition, the vibration is found to be large enough to dominate the unsteady flow field and a self-controlled vibration is induced.

For lock-in condition torsion mode, the vibration signal is virtually sinusoidal and the spectrum is sharply peaked, Figure 7. In this case, the shedding process is in phase along the span and the vibration amplitude significantly increases compared to lock-off conditions.

On the contrary, for lock-off condition and as mentioned by Blevins in a study on vortex shedding from cylinders [10], the vortex shedding is not a steady, harmonic, two-dimensional process. Vortex shedding does not occur at a single distinct frequency, but rather it wanders over a band of frequencies with a range of amplitude and it is not constant along the span. With the help of synchronized high speed visualization and laser vibrometer measurement, the spanwise variations in the flow and the corresponding vortex-induced vibration are evidenced in Figure 8. The time trace displays amplitude modulation and intermittent weak shedding cycles, which are typical of the occurrence of vortex dislocations, Szepessy et al. [11]. Indeed, the Figure 8 displays direct relation between the vortices spanwise organization and the vortex-induced vibration level: For parallel vortex shedding, the fluctuating force on the body is maximal and the vibration level is significantly increased. On the contrary, for 3D vortex shedding, the vortex-induced vibration level is reduced. According to such vortices spatial randomness, the hydrofoil vibration spectrum is broad band, Figure 14. Besides, the spectrum shows energy at the three hydro-elastic coupling frequencies but with significant level at the torsion eigen frequency, 900 Hz.
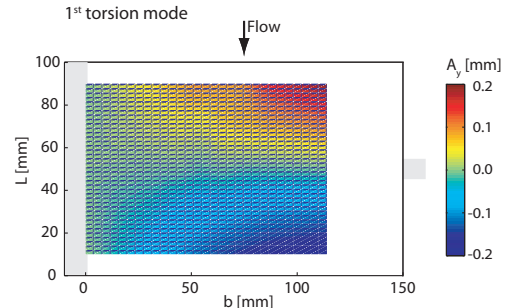

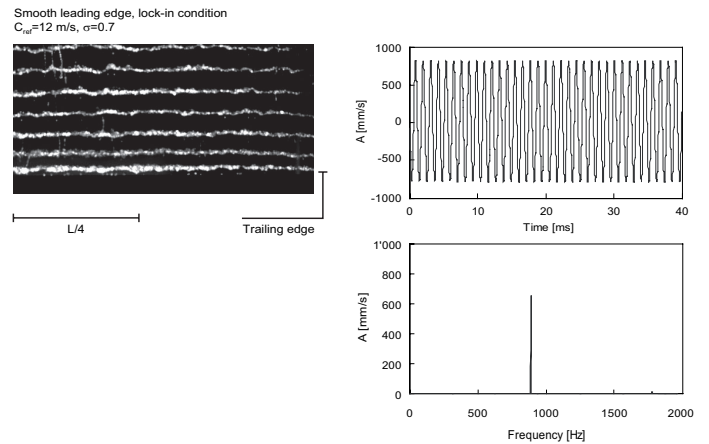Figure 6: Survey of the hydrofoil wall vibration amplitude for lock-in condition, C_{ref}= 12 m/s

Figure 7 : Top-view visualization of Kármán vortex street cavitation, vibration time signal and spectra for lock-in condition and smooth leading edge
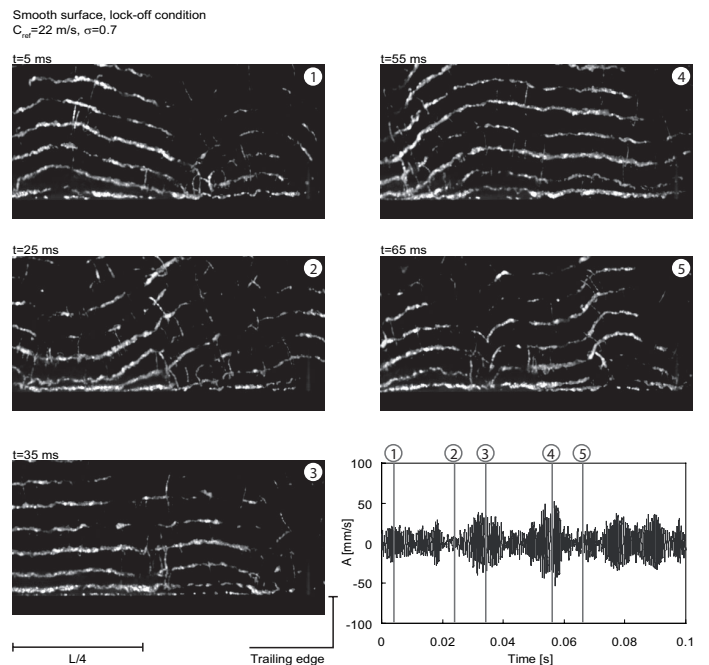

Figure 8 : Top-view visualization of Kármán vortex street cavitation and vibration time signal for lock-off condition and smooth leading edge

FLUID-STUCTURE INTERACTION FOR ROUGH LEADING EDGE

As above mentioned, Caron [8] evidences that the boundary layer transition to turbulence for the tested hydrofoil is located slightly downstream of the midchord for an incidence angle of 0° and the considered Reynolds number range. By placing a distributed roughness at the leading edge, the transition to turbulence is forced at this position. This section describes the effects of the boundary layer modification on the Kármán vortex shedding frequency, vortex-induced vibration and vortex generation process.

ROUGHNESS EFFECTS ON KARMAN SHEDDING FREQUENCY

The waterfall spectra of the laser vibrometer signals is presented in Figure 9 for different upstream velocities. In a similar way as the case with the smooth leading edge, the Kármán vortex shedding frequency increases linearly with the upstream velocity. For several conditions, significant increases of the vibration level reveal hydro-elastic couplings.
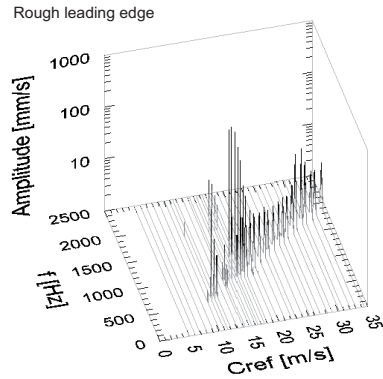

Figure 9 : Waterfall spectra of the laser vibrometer signals for different upstream velocities, cavitation free

The vortex shedding frequency is presented in Figure 10 as a function of the flow velocity and compared to the case with smooth leading edge. Again, a linear relationship between the vortex shedding frequency and the upstream velocity is observed provided that no hydrofoil resonance frequencies are excited. Nevertheless, the Kármán shedding frequency is significantly decreased. The mean Strouhal number value therefore decrease from 0.24 for the smooth leading edge to 0.18 for the rough one. Consequently, the torsion mode lock-in is also evidenced for the rough leading edge but at higher upstream velocities.
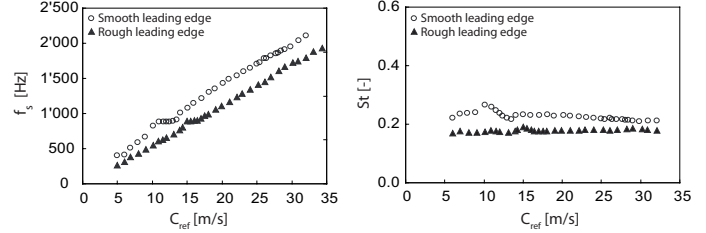

Figure 10 : Shedding frequency of Kármán vortices and Strouhal number for different upstream velocities and roughnesses, cavitation free

ROUGHNESS EFFECTS ON VIBRATION LEVEL

The standard deviation of the hydrofoil displacement velocity signal, which is band-pass filtered around the Strouhal frequency, is displayed on Figure 11 for different upstream velocities, lock-off regimes for both roughness configurations. Significant increase of the vibration level with the roughness is evidenced.
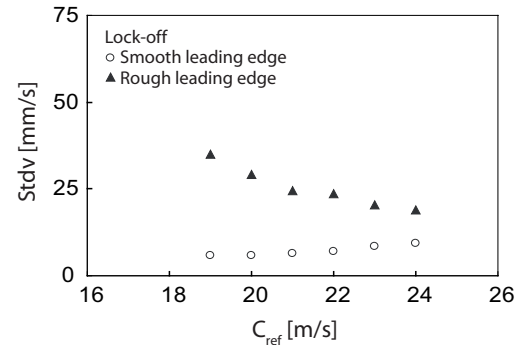

Figure 11 : Vortex-induced vibration level for different upstream velocities and roughness configurations, cavitation free

For a lock-off condition C_{ref}= 22 m/s, the vibration signal for smooth and rough leading edges are compared in Figure 12. The significant increase of the overall vibration level is evidenced. Moreover, the intermittent weak shedding cycles, corresponding to the low vibration level, are less frequent with the roughness. As a result, the spectra presented in Figure 13 are sharply peaked for the case with the roughness and broad band for the smooth one. The vibration amplitude at the shedding frequency is significantly increased with the roughness.
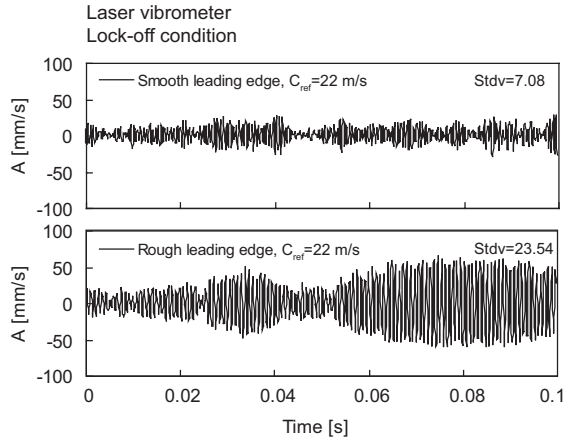
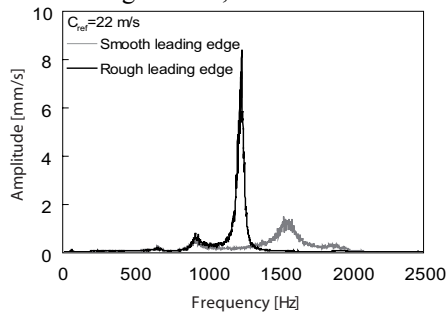Figure 12 : Vibration time signal for different roughness configurations, cavitation free

Figure 13 : Vibration signal spectra for different roughness, cavitation free

The modulation of the vortex-induced vibration signal is next considered. The vibration signals are low-pass filtered (5000 Hz) and the envelopes computed using the Hilbert function. The vibration signal, the envelope and their spectrum are presented in Figure 14 for a lock-off condition, C_{ref}= 22 m/s. The envelope spectrum reveals energy at low frequency but without any characteristic frequency. As a result, the occurrence of the weak shedding cycles, which correspond to vortex dislocations, is non-periodic. A form factor is defined as the standard deviation of the envelope signal scaled by the standard deviation of the vibration signal: Therefore, lock-in or hydro-elastic couplings lead to low form factor values as it tends to 1 for highly modulated signal. The form factor is plotted on Figure 15 for the smooth and rough leading edges and for different upstream velocities in lock-off regimes. The form factor is significantly decreased with the roughness. Consequently, with the roughness, the vortex-induced vibration signal is less modulated. The occurrence of the vortex dislocations is thus less frequent.
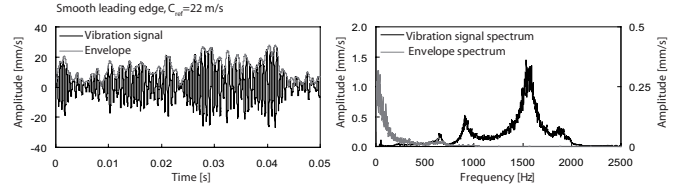

Figure 14 : Vibration signal, vibration signal envelope and their spectra for smooth leading edge and lock-off condition, cavitation free
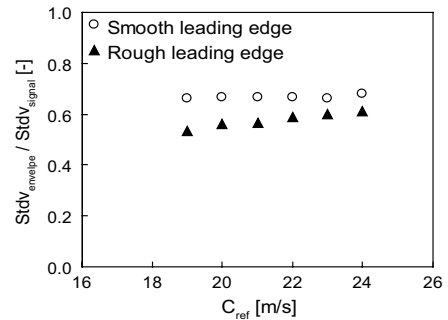

Figure 15 : Form factor of the vibration signal: Standard deviation of the envelope scaled by the standard deviation of the signal, cavitation free

ROUGHNESS EFFECTS ON VORTICES GENERATION PROCESS

Synchronized high speed visualization and laser vibrometer measurement is presented in Figure 16 for the rough leading edge. In comparison with Figure 8 for the smooth configuration, the overall vibration level is increased as well as the vortices spanwise organization. In this time window, the cavitation vortices exhibit 2D pattern except in the case of low vibration amplitude where vortices dislocations occur. This a fundamental change in the vortices generation process compare to the one with the smooth leading edge. For the latest, in the Figure 8 time window, the vortices cavitation exhibit essentially 3D pattern except in the infrequent case of high vibration amplitude where vortices 2D pattern is evidenced.

Obviously, the shedding process of the Kármán vortices is highly related to the state of the boundary layer over the entire hydrofoil. It is believed that in the case of smooth leading edge, the location of the transition to turbulence, which exhibits an unsteady 3D shape, has a direct influence on the wake structure. On the contrary, for the rough leading edge, the location of transition to turbulence is forced to occur at the leading edge, which leads to an enhancement of the coherence length of the Kármán vortices.

Rough leading edge, lock-off condition
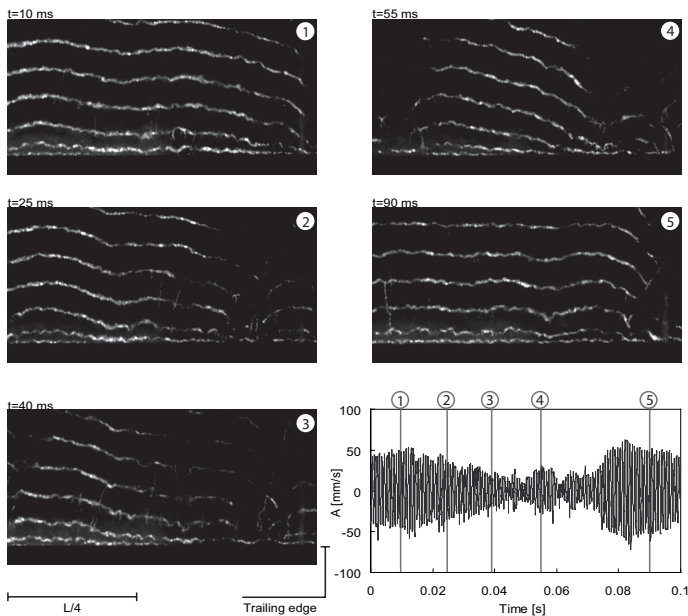C_{ref}=22 m/s, σ=0.6

Figure 16 : Top-view visualization of Kármán vortex street cavitation and vibration time signal for lock-off condition and rough leading edge

CONCLUSION

The present study deals with the shedding process of the Kármán vortices in the wake of a NACA0009 hydrofoil at high Reynolds number, Re_h=25·10^3 - 65·10^3. This research addresses the effects of the foil leading edge roughness on the wake dynamic with a special focus on the vortex shedding frequency, vortex-induced vibration and wake organization. Besides the smooth leading edge, a configuration of distributed roughness with an average values of 125 μm is investigated. The Kármán vortex street is also analyzed by synchronized high speed visualization and measurement of vortex induced vibration. Information about the correlation of the vortex coherent length and the vibration level is extracted.

For smooth leading edge, the shedding frequency of Kármán vortices occurs at constant Strouhal number, St=0.24. The wake exhibits 3D instabilities and the vortex induced vibration signals strong modulation with intermittent weak shedding cycles. Direct relation between vibration amplitude and vortex spanwise organization is shown. In the case of rough leading edge, the Kármán shedding frequency is notably decreased compared to the smooth one, St=0.18. Moreover, the vortex induced vibration level is significantly increased and the vibration spectra sharply peaked. The occurrence of vortex dislocations is shown to be less frequent with the roughness. The shedding of the vortices is considered on the whole as in phase along the hydrofoil span.

Obviously, the shedding process of the Kármán vortices is highly related to the state of the boundary layer over the entire hydrofoil. It is believed that in the case of smooth leading edge, the location of the transition to turbulence, which exhibits an unsteady 3D shape, has a direct influence on the wake structure. On the contrary, for the rough leading edge, the location of transition to turbulence is forced to occur at the leading edge, which leads to an enhancement of the coherence length of the Kármán vortices.

REFERENCES

[1] Achenbach E., Heinecke E., (1981), On vortex shedding from smooth and rough cylinders in the range of Reynolds numbers 6x10^3 to 5x10^3, J. Fluid Mech., 109:239-251

[2] Cheung J.C.K, Melbourne W.H., (1983), Turbulence effects on some aerodynamic parameters of a circular cylinder at supercritical Reynolds numbers, J. Wind Engng Ind. Aero., 14:399-410

[3] Blackburn H.M., Melbourne W.H., (1996), The effect of free-stream turbulence on sectional lift forces on a circular cylinder, J. Fluid Mech., 306:267-292

[4] Young J., Holl J. (1966), Effects of cavitation on periodic wakes behind symmetric wedges, J. Basic Engrg, 88:163-176

[5] Ausoni P., Farhat M., Escaler X., Avellan F., (2006), Cavitation in Kármán vortices and flow induced vibrations, Proc. Sixth International Symposium on Cavitation, Wageningen, The Netherlands

[6] Ausoni P., Farhat M., Escaler X, Egusquiza E., Avellan F., (2007), Cavitation influence on Kármán vortex shedding and induced hydrofoil vibrations, accepted for publication, J.Fluids Eng, Aug 2007

[7] Avellan F. et al. (1987), A new high speed cavitation tunnel, ASME Winter Annual Meeting, Boston (USA), 57: 49-60

[8] Caron J.-F., Farhat M., Avellan F. (2000), On the leading edge cavity development of an oscillating hydrofoil, ASME Fluids Engineering Division Summer Meeting, Boston (USA), FEDSM2000-11016

[9] Ait Bouziad Y. (2005), Physical modelling of the leading edge cavitation: Computational methodologies and application to hydraulic machinery, PhD thesis, EPFL, N^0 3353

[10] Blevins R.D. (1985), The effect of sound on vortex shedding from cylinders, J.Fluid Mech, 161:217-237

[11] Szepessy S., Bearman P.W. (1992), Aspect ratio and end plate effects on vortex shedding from a circular cylinder, J.Fluid Mech, 234:191-217